

/data1/ws/essay/pinegl/pineglas20070608.la.tex
plots in /data1/ws/essay/pinegl/plots/pineglasplots
backup in /data5/ws/essay/pinegl

**Elevation Changes in Pine Island Glacier, Walgreen Coast, Antarctica,
based on GLAS (2003) and ERS-1 (1995) Altimeter Data Analyses
and Glaciological Implications**

Ute C. Herzfeld¹, Patrick McBride¹, Jay Zwally², and John DiMarzio³

¹Cooperative Institute for Research in Environmental Sciences,
University of Colorado Boulder, Boulder, CO 80309-0449, USA
e-mail: Herzfeld@tryfan.colorado.edu

² Ice Branch, NASA Goddard Space Flight Center, Code 614.1, Greenbelt, MD 20771, USA

³ SGT Inc., NASA Goddard Space Flight Center, Code 614.1, Greenbelt, MD 20771, USA

Corresponding Author:

Ute Herzfeld
CIRES
University of Colorado Boulder
Boulder, Colorado 80309-0449
USA

e-mail: Herzfeld@tryfan.colorado.edu

phone: +1-303-735-5164

fax: +1-303-492-2468

ABSTRACT

The Geoscience Laser Altimeter System (GLAS) aboard ICESat, launched in January 2003, has been designed to detect and monitor changes in the cryosphere. The first objective of this paper is to present high-resolution ice-surface elevation maps derived from GLAS data, using geostatistical analysis. In a regional study of Walgreen Coast and Northern Ellsworth Land, West Antarctica, differences in the representation of geographic and morphologic features in maps based on ERS-1 radar altimeter data and on GLAS data are investigated, with the result that in particular in topographically complex coastal areas and the margin of the ice sheet the improvement in precision and accuracy of the laser altimeter is significant.

A second, applied objective is to map elevation changes in Pine Island Glacier, a glacier that plays a key role in the question of stability of the West Antarctic Ice Sheet and has been changing rapidly in recent years. Results of elevation differencing of 2003-GLAS-data and 1995-ERS-1-radar-altimeter-data DEMs (1) show that thinning rates have been increasing and (2) are applied to attribute the observed changes in Pine Island Glacier to internal processes in the glacier, related to dynamic thinning. More generally, this application serves to demonstrate that GLAS data facilitate study of cryospheric change.

Keywords: Satellite data, ice dynamics, cryospheric change, geostatistics, satellite data processing

(1) Introduction

The cryosphere is presently undergoing rapid changes, which may be linked to climatic warming. For example, outlet glaciers of the Greenland and Antarctic Ice Sheets are affected by surface lowering and front retreat, and the Arctic sea ice is melting. Changes in large and remote ice areas are best observed with the aid of satellite-remote sensing. ICESat, the Ice, Cloud and land Elevation Satellite, was launched on 13 January 2003 as part of NASA’s Earth Science Enterprise with the goal to obtain accurate elevation measurements, mainly of the Earth’s ice surfaces, using the Geoscience Laser Altimeter System (GLAS), and to monitor changes in the cryosphere (Zwally et al. 2002, Schutz et al. 2005).

The objectives of this paper are three-fold, including remote-sensing as well as glaciologic components:

- (1) to present high-resolution ice-surface elevation maps derived from ICESat GLAS data,
- (2) to study one of the most-rapidly changing outlet glaciers of the West-Antarctic Ice Sheet, Pine Island Glacier,
- (3) to compare digital elevation models (DEMs) based on GLAS laser altimeter data with DEMs derived from ERS-1 radar altimeter data
 - (a) to investigate the differences in representation of morphologic units in GLAS and ERS-1 data,
 - (b) to demonstrate that GLAS data may be utilized for cryospheric change detection, and
 - (c) to contribute to understanding the glaciologic processes related to the currently observed retreat of Pine Island Glacier.

As an introduction, we will provide background on both the remote-sensing component, focussing on satellite radar and laser altimeter observations (section (1.1)), and on the glaciologic application, which is centered around the fact that Pine Island Glacier has been considered a key glacier in the question of stability of the West-Antarctic Ice Sheet *and* is presently showing signs of rapid retreat (section (1.2)) — indicating that some of the predicted changes that may cause the entire ice sheet to collapse may now actually be happening. Hence this Antarctic glacier is a good example to demonstrate the importance of accurate elevation mapping and the capabilities of satellite-laser altimeter observations from ICESat.

The main parts of the paper will be organized as follows: In section (2), the properties of the ERS-1 satellite radar altimeter data used in the comparison and the properties of ICESat GLAS data will be described. The distribution patterns of satellite radar as well as laser altimeter data on the ground consist of discrete “spots” along ground tracks, whose spacing depends on the repeat in time, which in turn is specific to the satellite mission — in any case curvilinear diamond-shaped gaps of many kilometers remain between the ascending and the descending satellite ground tracks, and hence interpolation is necessary to obtain elevation models based on regular grids with a full coverage of the area of interest. Our approach is based on application of the geostatistical method in the form detailed in Herzfeld (2004) and summarized in section (3), where special attention will be given to problems of GLAS data interpolation and their solutions. As a first application, we shall derive an elevation map of Walgreen Coast, Antarctica, the region that encompasses Pine Island Glacier, from GLAS data. In a comparison with a map of the same area based on ERS-1 data, we will investigate the mapping capabilities of GLAS for different glacio-morphologic units (section 4). Finally (section 5), we will utilize the mapping capabilities derived in section (3) in a study of Pine Island Glacier and its changes, from ERS-1 and GLAS maps at a larger scale. The glaciologic and remote-sensing conclusions will be summarized and discussed in section (6).

(1.1) Remote-Sensing Introduction: Mapping Ice Elevations Using Satellite Altimetry

Radar altimeter observations of ice sheets go back to SEASAT (launched 1978), the first satellite to produce scientifically useful altimeter data. Although SEASAT was only operational for about 3 months (10 July

to 9 October, 1978), corresponding to late austral winter on the southern hemisphere, the existence of SEASAT radar altimeter data make this data type the oldest geophysical data for ice observation, which is relevant for monitoring changes. After SEASAT, GEOSAT (U.S. Navy Geodetic Satellite) was launched with a similar altimeter on board. The ERS-1 and ERS-2 satellites, operated by the European Space Agency (ESA), each carry a suite of instruments including a radar altimeter and a Synthetic Aperture Radar (SAR). ERS-1 and ERS-2 satellites also fly at 785 km above the Earth's surface, as did SEASAT and GEOSAT, in sun-synchronous orbits. ERS-1 collected altimeter data from July 1991 to May 1996, at which time the altimeter was shut off deliberately. ERS-2 started collecting radar altimeter (RA) data in August 1995. Other satellites that carry altimeters include JASON-1, JASON-2 and ENVISAT.

A new generation of altimeter observations of the Earth was started with the Geoscience Laser Altimeter System (GLAS) aboard ICESat, launched in 2003. The GLAS instrument has a smaller footprint and a higher accuracy than a radar altimeter. GLAS data and their properties will be further described in section (2.2).

Satellite radar altimeter data have been used as the primary source for mapping Antarctic ice surface elevations (eg. Herzfeld and Matassa 1999, Bamber 1994, Herzfeld et al. 2000, Herzfeld 2004). A brief introduction into the problems of and approaches to mapping ice elevations from radar altimeter data is in order, as a central focus of this paper is to derive an approach that works for GLAS data. The principles of mapping from radar altimeter data also apply to laser altimeter data, but with different numerical specifications of accuracy, precision and resolution, and with different instrument-performance characteristics.

All altimeter data follow ground track patterns with large gaps (depending on mission type) and are affected by slope, surface roughness and topographic relief, atmospheric conditions, but penetrate cloud cover. In the retracking process, elevation is associated with location on the ground (see, e.g., Martin et al. 1983, Brooks et al. 1983, Partington et al. 1987, Herzfeld 2004). In locations where the track crosses a cliff or other significant step in topography, such as the edge of an ice shelf or a steep mountain, the apparent location of the topographic step is incorrect ("snagging effect", Partington et al. 1987), and the apparent slope is lower than the actual slope. As a consequence, mapping of ice surfaces was restricted to regions of low slopes in earlier work (Partington et al. 1987, Bamber 1994). However, the more interesting marginal areas of the ice sheets, where outlet glaciers flow into the oceans, are also the areas of steeper slopes and more complex topography.

Using geostatistical methods with search routines specifically adapted to the track-line pattern of satellite altimeter data and special methods to estimate the spatial structure function of the data, it has been possible to map ice surfaces from radar altimeter data with sufficient accuracy for detection of the grounding line on Antarctic outlet glaciers and for glaciological modeling, as first demonstrated by Herzfeld et al. (1993, 1994). An atlas of DEMs and maps covering Antarctica (to the southern limit of altimeter data coverage, which is 72.1° S for GEOSAT and 81.5° S for ERS-1), has been published in book form and electronically by Herzfeld (2004, data available under <http://nsidc.org/data>). The Atlas DEMs provide a basis for monitoring changes in surface elevation. In this paper, we will utilize DEMs derived from 1995 ERS-1 RA data as the basis for comparison with GLAS data (see section (3)).

(1.2) Glaciological Introduction: The Role of Pine Island Glacier in Stability Scenarios for the West Antarctic Ice Sheet and Recent Changes

Antarctica has two large ice sheets, the East Antarctic Ice Sheet and the West Antarctic Ice Sheet (WAIS) (see Figure 1). While the East Antarctic Ice Sheet is generally considered stable, the stability of the geographically more divided and smaller chambered WAIS has long been a topic of discussion among glaciologists. The hypothesis of possible disintegration of the WAIS was first brought forward by Hughes (1973) and raised considerable interest because of its catastrophic outlook. Pine Island Glacier and the neighboring Thwaites Glacier, the two largest ice streams that drain the northern margin of the WAIS in Ellsworth Land and

Marie Byrd Land (see Figure 2), play an essential role in the instability scenario of the ice sheet, for the following reasons: Pine Island and Thwaites Glaciers are the fastest flowing glaciers in this part of Antarctica (Thwaites Glacier 2900 m yr^{-1} and Pine Island Glacier 2400 m yr^{-1} , after Ferrigno et al. 1998). In the literature, Pine Island Glacier and Thwaites Glacier are treated together as sharing the rare property of being large glaciers, which are grounded below sea level with an inland slope for large parts of their areas. These properties are important in disintegration models. The grounding line could retreat rapidly and migrate inland until ultimately the whole marine portion of the ice sheet would be converted into an ice shelf (cf. Weertman 1974).

Hughes (1973, 1981) and Thomas et al. (1979) suggested that the northern part of the ice sheet could already be collapsing. The exceptionally low ice surface gradient, which is obvious east of Pine Island Bay (see Fig. 2), might support this hypothesis. Other authors hold a more moderate outlook. Crabtree and Doake (1982) modeled the longitudinal profile of Pine Island Glacier using steady-state assumptions and found no evidence of instability. The possibility that collapse of the West Antarctic Ice Sheet may lead to rapid sea-level rise in the near future is discussed in Bentley (1997). Assessment of the potential contribution to sea-level rise in the Amundsen Sea varies (1.2 m from BEDMAP ice volume above sea level (Lythe et al. 2001) to zero because of absence of significant imbalance (Bentley and Giovinetto 1991)). A summary is also given in Vaughan et al. (2001). From comparison of 1973 and 1975 LANDSAT satellite images and 1966 aerial photographs, Swithinbank (1988) concluded 10 km retreat or calving.

While in the earlier literature Pine Island Glacier and Thwaites Glacier are treated jointly, they are actually different (1) with respect to their glacio-morphological situation, and (2) with respect to the significance of recently observed changes. The glacio-morphological units will be discussed in the section (3) on results from altimeter mapping.

The fact that Pine Island Glacier has been changing rapidly in recent years, while Thwaites Glacier has not changed much, motivates the emphasis on Pine Island Glacier in this paper (see section (5)). Retreat of the grounding line of Pine Island Glacier and increase in flow velocity has been observed from interferometric analysis of SAR data (Rignot 1998, 2002; Schmeltz et al. 2002, Rignot et al. 2002, Rabus and Lang 2003), changes in crevassing of the glacier and changes in the ice front are visible in satellite imagery (Bindschadler 2002, Ferrigno et al. 1998), ice surface elevation mapping indicates that the ice in the drainage basin is thinning (Shepherd et al. 2001). Thwaites Glacier exhibits much less activity (Ferrigno et al. 1998, Bamber and Rignot 2002).

The elevation models derived in this paper will be analyzed to study the distribution of elevation changes. In a glaciologic discussion, we will demonstrate that difference maps between 1995 ERS-1 data and 2003 GLAS data may be utilized to contribute to an attribution of the observed changes to climatic and glacio-dynamic processes (section (5)).

(2) Altimeter Data Sources

ERS-1 satellite radar altimeter data and GLAS (Geoscience Laser Altimeter System) satellite laser altimeter data are evaluated using geostatistical methods to derive digital elevation models for Walgreen Coast (Atlas map area) and for Pine Island Glacier.

(2.1) 1995 ERS-1 Radar Altimeter Data

ERS-1 satellite radar altimeter data from 6 months in 1995 (01 Feb – 01 Aug) are selected as comparison basis for this study, to avoid seasonal effects. The chosen time frame largely overlaps with that part of the ERS-1 mission during which data with the densest tracks were collected.

(2.2) 2003 Geoscience Laser Altimeter System (GLAS) Data from ICESat

Instrumentation

The Geoscience Laser Altimeter System (GLAS), the sole instrument aboard ICESat, is a next-generation space lidar. GLAS combines a precision surface lidar with a sensitive dual-wavelength cloud and aerosol lidar, emitting infrared and visible (green) laser pulses at 1064 nm and 532 nm wavelengths. The 1064 nm (infrared) laser channel is designed for measurements of surface altimetry and heights of dense clouds and the 532 nm (green) lidar channel for measurements of the vertical distribution of clouds and aerosols. More precisely, the GLAS laser produces a 1064 nm 40Hz pulse for altimetry and lidar, and a doppler crystal produces a 532 nm wavelength pulse, which yields a more sensitive determination of the vertical distribution of clouds and aerosols (Schutz et al. 2005, Zwally et al. 2002). Note that, other than a radar altimeter, the laser altimeter signal does not penetrate optically dense clouds (but thin clouds).

ICESat orbits at 600 km above the Earth's surface. The footprint of GLAS is approximately 65 m in diameter, and the "spots" illuminated on the Earth's surface are separated by 172 m in along-track direction. The echo pulse is accepted by a 1-m-diameter telescope, directed to an analogue detector, digitized by a 1-GHz sampler, along with a digitized record of the transmitted pulse. The digitized pulses constitute the waveform data, from which transmit and echo receive time are determined. From the resultant 2-way travel time, the range between the satellite and the Earth surface is calculated, and, using precision orbit determination based on GPS star tracking and post-processed improvement of the pointing accuracy of the laser, the elevation of a point on the surface is derived (after Schutz et al. 2005).

The GLAS instrument was developed at NASA Goddard Space Flight center in partnership with a science team from universities, government and industry. Ball Aerospace built the spacecraft. During each campaign, ICESat is operated by the University of Colorado Laboratory for Atmospheric and Space Physics (LASP). GLAS and ICESat data are initially processed by the ICESat Science Investigator-led processing system with support from the University of Texas, Center for Space Research. Once sufficiently corrected, processed and released, GLAS data are/ will be publicly available through the National Snow and Ice Data Center/ World Data Center for Glaciology A, University of Colorado Boulder (see <http://www.nsidc.org/data/icesat/>).

Measurement Campaigns and Data Products

In this section we provide technical information necessary to evaluate GLAS data for Antarctic elevation mapping and name criteria for selection of the data used in this paper. There are three identical GLAS instruments aboard ICESat for redundancy, simply termed Laser1, Laser2, Laser3 (each operating with both frequencies). Unfortunately, Laser1 stopped working after about 39 days of operation. Laser2 was employed next, and currently (March 2007) Laser3 is in operation. To extend mission life and to maximize the science return despite the unexpectedly short life time of the lasers, the laser is now always operated for a 33-day subcycle of an initially defined 91-day repeat cycle at a time, three times per year. Data from each of these observation periods are named after the laser instrument with which they were collected (L1, L2, L3), then A,B,C for the campaign, for instance, we use data from L2A in this paper.

Campaigns from Laser 1 and Laser2A also include 8-day repeat cycles. The cross-track resolution depends on the repeat cycle, and hence with the loss of the 91-day and 183-day repeat cycles, no geodetic-quality data have been collected. At 183-day repeat, the across-track spacing would be 15 km at the equator and 2.5 km at 80° latitude. At 33-day repeat, the across-track spacing is approximately 90 km at the equator and 15 km at 80° latitude.

Since all instrumentation operated at or near expected performance during campaign L2A (see Schutz et al 2005), we use data from campaign L2A. However, over sloped surfaces, an effective range bias occurred in certain situations, due to an error in alignment of the laser direction and the FOV (star tracker field of view) (Schutz et al. 2005).

Campaign L2A had a 8-day-repeat-cycle part (25 September 2003 to 4 October 2003) and a 33-day-subcycle-of-91-day-cycle part (4 October 2003 to 20 October 2003). While these data, collected in a 33-day subcycle of the 91-day repeat cycle, are the densest data available, there are still large gaps. The distribution of the data used in our analysis is shown in Figure 3, for global elevation product, abbreviated GLA06. The existing gaps call for powerful interpolation methods, to still obtain useful and detailed maps of outlet glaciers.

There are 15 different data products, which are derived for every campaign. For instance, product GLA05 contains the waveform data and other technical information, GLA06 contains elevation and related data. Other elevation products relevant for terrestrial ice research include Antarctic and Greenland Ice Sheet elevation product (GLA12) and land-surface altimeter data (GLA14), which differ in correction methods. After initially investigating GLA12, GLA13 (sea-ice altimeter data), GLA14, GLA05 and GLA06, the work in this paper is based on GLA06 and GLA05 data, because these lower-level products contain additional types of information useful to improve mapping results (see section 3.3).

Data corrections are, in general, improved or added also from one release to the next; however, before using any certain data product from a given campaign in a given release, it is advisable to first obtain information on the actual processing and correction status. The work presented in this paper uses release-18 data, which was the latest release available at time of processing. We then applied some additional corrections (see section 3.3).

A data-set property that is important for mapping is the coverage mask. Data products GLA12 and GLA14 have the same coverage mask, which in addition to terrestrial ice and land areas includes island, ice-shelf and coastal sea-ice areas. The latter three are also contained in the sea-ice altimeter data in GLA13 and in the ocean altimeter data in GLA15. The GLAS coverage mask is based on a different coastline definition than that of ERS-1 data, which gives the maps a very different appearance (notice e.g. that Thurston Island is “missing” on the ERS-1 map, and so are many islands near the western end of Walgreen Coast (see section 4)).

(3) Geostatistical Methods for Analysis of Altimeter Data

(3.1) Principles

As noted in sections (1) and (2), altimeter data require interpolation because of the gaps in the data distribution, illustrated by Figure 3. The interpolation method applied here is ordinary kriging, in the form adapted for analysis of geophysical trackline data, and, in particular, satellite altimeter data, described in detail in Herzfeld (2004) (see also Herzfeld 1992, Herzfeld et al. 2000). Kriging methods are methods of geostatistical *estimation*, commonly formulated in a probabilistic framework, corresponding to geostatistical *interpolation and extrapolation* in the language of numerical analysis. In a situation of track patterns as in Figure 3, only *interpolation* is necessary to derive a digital elevation model. The method proceeds by two steps (1) variography, and (2) interpolation. In step (1), an analysis of the spatial structure of the data is carried out, experimental variogram functions are calculated and then variogram models are derived, which in turn provide input values for the second step, the interpolation. The estimation is based on an unbiased least-squares minimization, where assumptions about the degree of stationarity of the variable (here: elevation) or underlying trends can be entered in the unbiasedness conditions. Oftentimes, only step (2) is referred to as “kriging”, but step (1) is the essential step that renders realistic topographic maps, if the spatial surface roughness of the study area is represented correctly. Selection of a good variogram model requires experience in geostatistical data analysis, an understanding of data artefacts and geophysical knowledge of spatial properties of the variable and area under study.

In the analysis of GLAS data, variograms were derived for 6 different subareas of the Walgreen Coast area: (1) Pine Island Glacier, tongue and ice shelf, (2) Lower Pine Island Glacier, (3) Middle Pine Island Glacier, (4) Pine Island Glacier basin, (5) Thwaites Glacier basin, and (6) Lower Thwaites Glacier, including tongue.

Maps were made using 3 variogram models and a number of kriging parameter combinations.

(3.2) Atlas Mapping Scheme

To investigate the differences in representation between morphologic units encountered in the Antarctic Ice Sheet in ERS-1 and GLAS data (objective (3a)), we first study a regional map, of Walgreen Coast. The comparison is facilitated by using the same map boundaries as in the Antarctic Atlas. The Antarctic Atlas map tiling scheme has been designed such that each area in Antarctica (north of 81.5° , the limit of ERS-1 coverage) is on at least one map, along with a surrounding neighborhood, to avoid edge effects and related inconveniences (Herzfeld 2004). The Walgreen Coast map is bounded by geographic coordinates ($243\text{-}279^\circ$ E, $71\text{-}77^\circ$ S), and the Walgreen Coast map tile defined as the area rectangular in UTM coordinates inscribed in the area bounded by geographic coordinates, when transformed to UTM using central meridian 261° E (cf. Fig. 2.) The DEMs derived in this paper as well the the ones in the Antarctic Atlas have a grid spacing of 3 km. Elevations are referenced to WGS84.

(3.3) Problems of GLAS Data Interpolation and Their Solutions

Results of a first mapping of ice elevations from GLAS for the Walgreen Coast map tile (Figure 4) were disappointing, as all maps exhibited large artefacts, apparently related to track patterns in location. The existence of artefacts is based on errors in elevation of several hundred meters, which stands in contrast to reported high accuracy of GLAS data. Evaluating selected data over the Antarctic ice sheet, with clear sky conditions and low slope, the accuracy of release-21 data has been determined as 2.1 cm and the relative accuracy of elevations as 14 cm based on cross-over differences (Shuman et al. 2006). Fricker et al. (2005) report that elevation changes of 1.5 cm can be detected in GLAS data collected over a salt flat (Salar de Uyuni, Bolivia). An accuracy of a few centimeters was also established in a perfectly flat test area in White Sands, New Mexico, U.S.A., increasing to tens of centimeters for sloped areas associated with the pointing error (R. Schutz, pers. comm. 2005).

However, for areas of complex topographic relief, this accuracy does not hold, as the map in Figure 4 shows. In locations where the ERS-1 map of Walgreen Coast (Fig. 2) shows the Thwaites Glacier Tongue, the map in Figure 4, based on all GLAS data of campaign L2A, shows elevations of ≈ 800 m. The likely reason for these incorrectly high elevations is the presence of a small mountain range that trends north-south and is located south-southwest of the Thwaites Glacier terminus. The errors are likely attributable to problems in determination of the correct footprint location of a received signal (so-called snagging effect, Partington et al. 1987). Similar artefacts exist over Pine Island ice shelf, in both the presented map based on GLA06 data and a map based on the ice-elevation product GLA12. Lower Pine Island Glacier and the ice shelf in Pine Island Bay are also obstructed by huge errors. As expected, changing interpolation parameters even drastically did not remedy the situation much. Data need to be corrected in areas of high-relief topography.

A map based on the last 33 days of the Laser2A phase was created, as there were some acquisition disturbances during the first days of that phase. The resultant map (Fig. 4) shows Pine Island Glacier properly (except for a small artefact), but artefacts over Thwaites Glacier remain problematic.

Good results were achieved with a corrected data set, derived from a combination of data in GLA06 with information from data in the lower-level product GLA05 (waveform product), which includes technical information (a data point in GLA06 was rejected, if the received gain value of the matching record in GLA05 exceeded 50). A Gaussian variogram model with nugget effect 350 m^2 , sill 3450 m^2 and range 6000 m was used in the kriging inversion step. The resultant map is shown in Fig. 5. Pine Island Glacier and Thwaites Glacier areas are now free of artefacts, and the map can be utilized for a comparison with the ERS-1 map (section (4)) as well as for glaciologic analysis (section (5)).

(4) Comparative Description of Geographic, Morphologic and Glaciologic Features on the ERS-1 Map and the ICESat/GLAS Map of Walgreen Coast

The large geographical units shown on the maps of Walgreen Coast (Fig. 2 for ERS-1 radar altimeter data and Fig. 5 for ICESat GLAS data) are northeastern Marie Byrd Land, bordered here by Walgreen Coast, and northwestern Ellsworth Land, east of the longitude of Pine Island Bay. Cape Waite ($72^{\circ} 44'S/103^{\circ} 16'W$) on King Peninsula is the northeastern tip of Ellsworth Land and the northeasternmost continental land of the Amundsen Sea sector of Antarctica. Eights Coast, extending from Cape Waite east to Pfrogner Point ($72^{\circ} 37'S/89^{\circ} 35' W$) on Fletcher Peninsula, and Bryan Coast, extending east from Pfrogner Point, are the coasts of Ellsworth Land in our map area. The Walgreen Coast maps in Figures 2 and 5 show the drainage of Pine Island Glacier and the northern part of the Thwaites Glacier drainage, and westerly adjacent glaciers.

Abbot Ice Shelf borders much of Eights Coast. The ice shelf is well-mapped on the GLAS map, and less accurately on the ERS-1 map. North and east of Cape Waite is Thurston Island, a mountainous island (Walker Mountains), seen at 400-800 km UTM east on the northern edge of the GLAS map. In the small ice shelf between Thurston Island and Eights Coast is Sherman Island, which causes artefacts in track directions. Thurston Island is not shown on the ERS-1 map, which is attributed to the definition of the land masks that define the area of Antarctica and are different for ERS-1 data and GLAS data. The definition of the coast line is a non-trivial part of mapping Antarctica. East of Fletcher peninsula lies a small ice shelf, Venables Ice Shelf, which extends to Allison Peninsula on Bryan Coast. ICESat maps the ice shelf elevations more precisely, as inland ice flowing into the ice shelves and resulting in higher elevations is visible in the GLAS map.

Even in locations that are apparently inside the ERS-1 and the GLAS landmasks, there are eye-catching differences in the representation of the coastline and near-coastal areas in the GLAS map and the ERS-1 map. Comparison with a RADARSAT map (Jezek et al. 1999) and the USGS Satellite Image Map of Antarctica (Ferrigno et al. 1996) reveals that the ICESat map, while still problematic in some coastal areas—there are artefacts along the northern coast and on Thurston Island—, is surprisingly correct. Martin Peninsula with Cape Herlacher ($73^{\circ} 52'S/114^{\circ} 12'W$), the point that formally marks the boundary between Bakutis Coast and Walgreen Coast (at the left edge of this map) is captured. Bear Peninsula ($74^{\circ} 35'S/111^{\circ} W$) appears as an island between Dotson Ice Shelf ($74^{\circ} 24'S/112^{\circ} 22'W$) and Crosson Ice Shelf ($74^{\circ} 57'S/109^{\circ} 30' W$); and Moore Dome at the NW point of Bear Peninsula is discriminable. The half of the peninsula is very low. Notice that on the ERS-1 map in Figure 2, Bear Peninsula is not mapped at all (the area lies outside of the coastline boundary).

The high point south of Bear Peninsula is Mount Murphy ($75^{\circ} 20'S/110^{\circ} 44'W$, 2705 m), i.e. it is not an artefact (the elevation is mapped too low, as typical for altimetry, but the peak is in the correct location). Smith Glacier ($75^{\circ} 05'S/112^{\circ} W$) passes between Bear Peninsula and Mount Murphy, its main flow drains into Crosson Ice Shelf. Smith Glacier is a 160 km long, low-gradient glacier. The low elevation of 100 m to 40 m lets Bear Peninsula appear as an island optically. Kohler Glacier ($74^{\circ} 55'S/113^{\circ} 45'W$), a northern distribution of Smith Glacier, passes through the Kohler Range ($75^{\circ} 05'S/114^{\circ} 15'W$) and flows north, terminating in Dotson Ice Shelf. Some ice of Smith Glacier appears to flow north-northwest into Dotson Ice Shelf. An enlargement of this area may be necessary to study the glaciers west of Thwaites Glacier. With careful scrutiny, one may distinguish Pope Glacier, Vane Glacier, and Haynes Glacier, which points out the amazing detail that may be discovered with GLAS data. These glaciers are only of local importance and do not play a role in the instability question of the West Antarctic Ice Sheet. (Place names and geographic references after Alberts 1995).

Notably, the ice shelves show up nicely. Since Pine Island Glacier basin shows no more artefacts, we can use this map to investigate the initially posed question of changes in Pine Island Glacier.

The 1995 map of Walgreen Coast ice elevations based on ERS-1 altimeter data (Fig. 2) and GLAS data

(Fig. 5) shows Pine Island Glacier and Thwaites Glacier as two outlet glaciers with different glaciological and glacio-morphological units: Pine Island Glacier enters a sheltered bay with a small ice shelf, whereas Thwaites Glacier has a glacier tongue and an iceberg tongue which extend far into the ocean. The hinterland of the two glaciers is also morphologically different: Pine Island Glacier occupies a large trough that extends far inland and has a very low surface gradient, whereas Thwaites Glacier terminates on a steep section of Walgreen Coast. Some of these features are also depicted in satellite imagery published by Swithinbank (1988, figs. 92 and 93), Bindschadler (2002), and Ferrigno et al. (1998).

Pine Island Glacier appears to drain the entire area south of the coastal volcanic ranges that border the northern coast of Ellsworth Land. The high elevation area at (660,000 E/-8180,000 N) UTM indicates the Jones Mountains, the easternmost range of the volcanic province that extends to the Fosbick Mountains at 145° W (for UTM coordinates, cf. section (3.2)).

The surface gradient of Pine Island Glacier is lowest between 800 m and 700 m of elevation, and steeper above 800 m. Below 700 m, the surface steepens significantly to the coast, even in the center of the basin (Herzfeld 2004). The gradient is 200 m in 150 km between 600 and 800 m elevation (0.13% slope $\equiv 0.076^\circ$) on both the ERS-1 and the GLAS maps. But the gradient between 200 and 400 m elevation is 200 m in 15 km (1.3% slope $\equiv 0.76^\circ$) on the 1995 ERS-1 map and 200 m in 20 km (1% slope $\equiv 0.57^\circ$) on the 2003 GLAS map. This may be related to the thinning of Pine Island Glacier (see Section 4). According to Crabtree and Doake (1982), the drainage basin of Pine Island Glacier is $214,000 \text{ km}^2 \pm 20,000 \text{ km}^2$ and mass flux at the ice front is 25 ± 6 gigatons, equal to 28 km^3 , per year.

The glacio-morphologic differences present some indicators that changes in Pine Island Glacier and Thwaites Glacier may be driven by different processes, which indicates a separate analysis and different treatment in models may be worthwhile. In fact, the present rapid retreat of Pine Island Glacier compared to the small changes in Thwaites Glacier are already manifestations of the different sensitivity.

In summary, the inland areas of the Antarctic ice sheet are well-mapped by both ERS-1 radar altimetry and GLAS. Due to differences in the land mask defining the area of Antarctica, Thurston Island is not on the ERS-1 map. ICESat maps coastal areas more realistically than ERS-1 RA. Some of the typical effects of altimetry mapping are still apparent in the GLAS data-map, but are smaller than on the ERS-1 map, for instance, snagging of high-elevation points in areas of high topographic relief still creates along-track artefacts of too high elevations; the difference in size of the artefacts may be attributed to the higher precision and smaller footprint of the laser compared to the radar altimeter. The outlet glaciers, in particular Pine Island Glacier and Thwaites Glacier, have a sufficiently low gradient and smooth surface to be well-captured in both the ERS-1 and the GLAS-data maps, after geostatistical interpolation. As an application, an analysis of the changes in Pine Island Glacier is warranted (section (5)).

(5) Pine Island Glacier Study

The following analysis is based on maps of lower Pine Island Glacier and the ice shelf in Pine Island Bay, derived from a 1995 ERS-1 elevation model (see Fig. 6), and a 2003 GLAS elevation model (see Fig. 7). The GLAS model for Pine Island Glacier is calculated using the same data processing and geostatistical estimator as the model that underlies Figure 5. A difference map, showing elevation differences in the form (GLAS(2003)–ERS-1) is presented in Figure 8, with ERS-1 contours in the style of the Antarctic Atlas (cf. Fig. 2 or 6a) superimposed for ease of comparison.

On the ERS-1 map, the offshore part of Pine Island Glacier is seen to increase the elevation by 10–20 m over the surrounding ice shelf.

Grounding line. The location of the 50 m contour (above WGS84) on the Atlas detail map of Pine Island Glacier matches the location of the grounding line determined from ERS-1 radar interferometry (Schmeltz

et al. 2002). Criteria for determination of the grounding line from DTMs are (1) break-in-slope criterion: grounded ice above the break in slope, floating ice below the break in slope; (2) surface-roughness criterion: smooth surface of floating ice, rough surface of grounded ice. A break in slope exists at the 50 m contour line. Another less significant break in slope is at the 80 m contour line. From the contours it appears that the grounding line is between the 50 m contour and the 60 m contour. The roughness criterion is also met at the 50 m contour. The 40 m contour approximately outlines the location of the floating tongue of Pine Island Glacier protruding into Pine Island Bay. The grounded Pine Island Glacier extends 30 km into Pine Island Bay (measured from a line connecting points on the north and south side of the glacier margin on the detail map). In Schmeltz et al. (2002) the grounding-line-to-front distance is about 40 km. The front is not determined well in radar altimeter data in general (Partington et al. 1987), so this is a fairly good correspondence. In contrast, the 1400 m sounding that marks the location of the grounding line in Crabtree and Doake (1982) is located much further upglacier (80 km from the front), this location is supported in Swithinbank (1988) in an analysis of a LANDSAT1MSS image (1973).

The area that consists of the grounded part of the glacier tongue in 1995 has significantly lost in thickness by 2003 (to 25 m) (Fig. 8). The entire feature of concentric contour lines has shortened and retreated (Fig. 7a (GLAS) compared to Fig. 6a (ERS-1)). This indicates a retreat of the grounding line by about 20 km. Even if this feature is not the grounding line, the glacier has retreated approximately 20 km. The thickness of the ice shelf is also lower. The floating tongue part, marked by elevated surface heights, has receded; it is narrower in the front (≈ 80 km wide on the ERS-1 map (Fig. 6b), 10 km wide on the GLAS map (Fig. 7b) at (445 km E/-8335 km N)) and wider at 460 km UTM East (150 km on GLAS map, Figure 7b). The “zero” outlines, which appear as overdeepenings, may be areas devoid of shelf ice or the results of topographic effects in altimeter data (see Herzfeld et al. 1993). Notably, on the GLAS map the latter are no longer present. The ice front location is similar in both maps; however, the location of the ice front is not typically well-depicted in altimetry, and better in SAR data or satellite imagery. The location of the 20-m contour has receded, indicating loss of mass in the ice shelf. Elevations in the ice-shelf part close to the coast have not changed much.

Difference Map: Distribution of Elevation Changes in Pine Island Glacier and Conclusions on Glaciologic Processes

Background:

Modeling and data analysis work on Pine Island Glacier is ongoing reflecting the importance of the problem of the presently observed rapid changes in the glacier. There is still a wide range of possible explanations for glaciodynamic processes that may explain the observations. Our first objective here is to quantify and map the distribution of elevation changes that occurred between 1995 and 2003. The second objective is then to contribute to an explanation of the likely causes of such changes. For the second topic, we need some background:

The changes in Pine Island Glacier may be caused by *external forcing* (A) or *internal forcing* (B):

- (A) In an *external-forcing scenario*, break-up of part of the ice shelf in Pine Island Bay leads to loss of back-holding power that affects Pine Island Glacier. As a result, the glacier accelerates, first the parts that are closest to the grounding line. Vieli and Payne (2004) analyze how events in the ice shelf may lead to changes in the glacier and support an external-forcing hypothesis.
- (B) In an *internal-forcing scenario*, changes in the glacier or in its accumulation basin explain elevation and thickness changes. These may or may not affect the ice shelf. Changes in the glacier may have dynamical causes (acceleration) or climatic causes (changes in accumulation, or increase of surface melting). Rabus and Lang (2003) support an internal-forcing hypothesis and attribute observed break-off of large icebergs off the ice shelf to chance.

Observations:

The most pronounced feature in the difference map (Figure 8) is a half-ring of significant surface lowering in the inland part of lower Pine Island Glacier basin, as mapped by light-green color (-50 to -100 m) and solid green color (-25 to -50 m). In some areas, thinning exceeds 100 m. The observed thinning decreases in upglacier direction and in upward direction in the drainage basin (outward from the half-ring). At elevations of 600–800 m, areas of thinning are interspersed with areas of 0–25 m thickening; the thinning areas are about twice as large in area as the thickening areas, hence on average the lower Pine Island Glacier has lost more than 50 m. The area on the ice shelf that in 1995 showed higher elevations where the center of the ice stream entered (the ice tongue protruding into the shelf area) has lost elevation by 25–20 m, the onlapping tongue is much shorter and shallower in the GLA map than in the ERS-1 map.

The color scheme of the difference map (Figure 8) is selected such that red on both ends of the scale indicates possibly untrustworthy data. The high of 200 m occurs in an area where the margin of the small ice shelf may be wrongly represented on the ERS-1 map. The low of -200 to -300 m is situated on a ridge descending from the Hudson Mountains, where the accuracy of the topography may be questionable. However, elevation losses of 150 m were, for instance, observed on Bering Glacier during the 1993–1995 surge (Herzfeld, 1998); which indicates that large changes in elevation are realistic during phases of dynamic changes of a glacier.

The signals of surface lowering, and in some areas, surface heightening, in the difference map are so large that improvements of the accuracy of GLAS data in later releases are comparatively negligible, as the accuracy of ERS-1 data is 3 cm and that of GLAS data also in the centimeter - lower decimeter range, including errors of pointing accuracy that were improved later. The accuracy of elevation differences between ERS-1 and GLAS data is hence on the order of a few centimeters to few decimeters. On the other hand, the following interpretations are valid even if absolute difference values would have several meters of error.

Interpretation and Results:

The observations of elevation-change distribution indicate dynamic thinning, which is internally forced: From the location and distribution of the areas of largest thinning, we conclude that the elevation changes are initiated in the glacier (internal forcing). A possible reason is acceleration of the glacier (dynamic thinning); one possibility is a dynamic wave that propagates down the glacier. The most plausible cause appears to be acceleration in the glacier, which is currently largest in the lower regions where the observed thinning is greatest. According to Rabus and Lang (2003), an acceleration with an amplitude of 12% of the Pine Island Glacier surface velocity extends 80 km upglacier from the grounding line (in the determination of Schmelz et al. 2002), which coincides with the area of surface lowering detected by our analysis. In the difference map (Fig. 8), surface lowering extends at least to 700 m elevation.

A change in accumulation rate is a less likely explanation, as in that case one would expect a surface lowering in the upper glacier basin and a more uniform distribution of surface lowering throughout the study area (the basin is mapped to 800 m elevation). If the surface lowering distribution were to be explained entirely by accumulation change, then in conclusion a decrease in accumulation a long time ago and an increase in more recent times would have to be postulated. As accumulation-caused changes travel much slower down-glacier than dynamic changes, one would not expect to see changes of this size and spatial distribution.

In conclusion, dynamic change remains the most plausible explanation. Hence with this work we are able to derive an answer to the question of internal versus external forcing of the changes in Pine Island Glacier.

Notably, the processes observed here are different from those in the Larsen Ice Shelf (B) break-up, which is clearly a case of external forcing and one that was climatically driven. In summary, different processes are responsible for the dramatic changes that occur in the Antarctic ice.

Shepherd et al. (2001) have reported a surface lowering of 1.5 m a^{-1} for 1992–1999 close to and upward of the grounding line. Our results indicate much larger thinning rates (3.125 m yr^{-1} for 25 m difference,

6.25 m yr⁻¹ for 50 m, and 12.5 m yr⁻¹ for 100 m). Even with the lowest rate, thinning has increased considerably in the past years. This process may be continuing.

(6) Summary and Conclusions

Mapping of Antarctic ice-surface elevations using satellite radar altimetry from ERS-1 and laser altimetry from the Geoscience Laser Altimeter System (GLAS) aboard ICESat is the primary objective of this paper. A second goal of the paper is the application in a glaciologic study of an Antarctic outlet glacier, demonstrating the usefulness of GLAS data as a means for measuring cryospheric change.

Principles of altimeter data collection from satellites are described, with particular emphasis on GLAS, covering instrumentation, data accuracy, data products and GLAS-specific terminology. GLAS data provide unprecedented accuracies in elevation mapping over ice surfaces from satellite, once technical difficulties are overcome. While accuracy in flat areas is in the centimeter-range, mapping of topographically complex areas requires special postprocessing. For derivation of digital terrain models of Antarctic surface elevations, geostatistical interpolation is applied.

A comparison of a GLAS map with an ERS-1 map of Walgreen Coast and Northern Ellsworth Land, West Antarctica, reveals different mapping capabilities of the ERS-1 radar altimeter and the GLAS instrument. While inland areas of the West Antarctic Ice Sheet are well-represented in both data sets, the improvement in precision and accuracy of the GLAS instrument over high-relief coastal areas and margins of the ice sheet is significant. In particular, glaciers and ice shelves along Walgreen Coast from Cape Herlacher to Pine Island Bay and along northwestern Ellsworth Land are well-mapped, which facilitates glaciologic studies.

As ICESat was designed to monitor changes in the cryosphere, we have carried out an application for Pine Island Glacier, a glacier that plays a key role in the question of stability of the West Antarctic Ice Sheet and that has been changing rapidly in recent years. A second set of maps is derived for the detailed study of Pine Island Glacier, which terminates on Walgreen Coast. Comparison of a map based on 2003 GLAS data to a map derived from 1995 ERS-1 radar altimeter data clearly indicates mass loss in large parts of lower Pine Island Glacier and Pine Island basin, and far less change in the floating part of Pine Island Glacier tongue and the ice shelf in Pine Island Bay. Thinning rates are larger than previously reported in the literature, which indicates that thinning rates are currently increasing.

The results of elevation differencing between 2003 GLAS and 1995 ERS-1 DEMs can be applied to answer an open glaciologic question, which concerns the processes that potentially cause the observed elevation changes. From the spatial distribution of the areas of largest thinning, we conclude that the changes in Pine Island Glacier are caused by internal processes in the glacier, related to dynamic thinning.

More generally, the Pine Island Glacier study demonstrates that ICESat GLAS data may be used for cryospheric change detection and analysis.

Acknowledgements: Thanks to R. Schutz, University of Texas, for communication on ICESat GLAS data accuracy, and to R. Thomas, EG&G, NASA Wallops Flight Facility, for discussion of the topographically induced artefacts in the GLAS data. Thanks to R. Parker, Institute of Geophysics and Planetary Physics, Scripps Institution of Oceanography, for a new subroutine for his plotting software *color*, *contour* utilized in mapping. Work funded by NASA Cryospheric Sciences Program under grant NNG04G062G to UCH.

REFERENCES

- Alberts FG (1995) (ed) Geographic names of the Antarctic. U.S. Geological Survey, U.S. Board on Geographic Names, Reston, VA
- Bamber JL (1994) A digital elevation model of the Antarctic Ice Sheet, derived from ERS-1 altimeter data and comparison with terrestrial measurements. *Annals of Glaciology* 20: 48-53.
- Bamber J, Rignot E (2002) Unsteady flow inferred for Thwaites Glacier, and comparison with Pine Island Glacier, West Antarctica. *Journal of Glaciology* 48(161): 237-246
- Bentley CR (1997) Rapid sea-level rise soon from West Antarctic ice sheet collapse? *Science* 275: 1077-1078.
- Bentley CR, Giovinetto MB (1991) Mass balance of Antarctica and sea level change. In: Weller G, Wilson CL, Severin BAB (eds) International Conference on the Role of the Polar Regions in Global Change: proceedings of a conference held June 11-15, 1990 at the University of Alaska Fairbanks, vol II: 481-488. University of Alaska, Geophysical Institute/Center for Global Change and Arctic System Research, Fairbanks, AK
- Bindschadler RA (2002) History of lower Pine Island Glacier, West Antarctica, from Landsat imagery. *Journal of Glaciology* 48(163): 536-544
- Brooks RL, Williams RSjr, Ferrigno JG, Krabill WB (1983) Amery ice shelf topography from satellite radar altimetry. In: Oliver RL, James PR, Jago JB (eds) Antarctic earth science. Australian Academy of Science, Canberra, and Cambridge University Press, Cambridge, pp 441-445
- Chelton DB, Ries JC, Haines BJ, Fu L-L, Callahan PS (2001) Satellite altimetry. In: Fu L-L, Cazenave A (eds) Satellite altimetry and earth sciences. Academic Press, San Diego, pp 1-131
- Crabtree RD, Doake CSM (1982) Pine Island Glacier and its drainage basin: results from radio echo-sounding. *Annals of Glaciology* 3: 65-70
- Ferrigno JG, Mullins JL, Stapleton JA, Chavez PSjr, Velasco MG, Williams RSjr, Delinski GFjr, Lear D'A (1996) Satellite image map of Antarctica. United States Geological Survey Miscellaneous Investigations Series Map I-2560, 1:5 000 000 scale
- Ferrigno JG, Williams RSjr, Rosanova CE, Lucchitta BK, Swithinbank C (1998) Analysis of coastal change in Marie Byrd Land and Ellsworth Land, West Antarctica, using Landsat imagery. *Annals of Glaciology* 27: 33-40
- Fricker HA, Borsa A, Minster B, Carabajal C, Quinn K, Bills B (2005) Assessment of ICESat performance at the salar de Uyuni, Bolivia. *Geophysical Research Letters* 32 (L21S06), doi: 10.1029/2005GL023423
- Herzfeld UC (1992) Least squares collocation, geophysical inverse theory, and geostatistics: A bird's eye view. *Geophysical Journal International* 111(2): 237-249
- Herzfeld UC (1998) The 1993-1995 surge of Bering Glacier (Alaska) — a photographic documentation of crevasse patterns and environmental changes, *Trierer Geograph. Studien*, 17, 211 pp., Geograph. Gesellschaft Trier and Fachbereich VI – Geographie/Geowissenschaften, Universität Trier
- Herzfeld UC (2004) Atlas of Antarctica. Topographic maps from geostatistical analysis of satellite radar altimeter data. Springer, Berlin, 364 pp
- Herzfeld UC, Matassa MS (1999) An atlas of Antarctica north of 72.1° S from GEOSAT radar altimeter data. *International Journal of Remote Sensing* 20: 241-258.
- Herzfeld UC, Lingle CS, Lee L-h (1993) Geostatistical evaluation of satellite radar altimetry for high resolution mapping of Lambert Glacier, Antarctica. *Annals of Glaciology* 17: 77-85
- Herzfeld UC, Lingle CS, Lee L-h (1994) Recent advance of the grounding line of Lambert Glacier, Antarctica,

- deduced from satellite radar altimetry. *Annals of Glaciology* 20: 43–47
- Herzfeld UC, Stosius R, Schneider M (2000) Geostatistical methods for mapping Antarctic ice surfaces at continental and regional scales. *Annals of Glaciology* 30: 76–82.
- Hughes T (1973) Is the West Antarctic ice sheet disintegrating? *Journal of Geophysical Research* 78(33): 7884–7910
- Jezek KC, Liu H, Zhao Z, Li B (1999) Improving a digital elevation model of Antarctica using radar remote sensing data and GIS techniques. *Polar Geography* 23(3): 185–200.
- Lythe MB, Vaughan DG, BEDMAP Consortium (2001) BEDMAP: a new ice thickness and subglacial topographic model of Antarctica. *Journal of Geophysical Research* 106(B6): 11335–11351
- Martin TV, Zwally HJ, Brenner AC, Bindschadler RA (1983) Analysis and retracking of continental ice sheet radar altimeter waveforms. *Journal of Geophysical Research* 88(C3): 1608–1616
- Partington KC, Cudlip W, McIntyre NF, King-Hele S (1987) Mapping of the Amery Ice Shelf, Antarctica, surface features by satellite altimetry. *Annals of Glaciology* 9: 183–188
- Rabus BT, Lang O (2003) Interannual surface velocity variations of Pine Island Glacier, West Antarctica. *Annals of Glaciology* 36: 205–214
- Rignot EJ (1998) Fast recession of a West Antarctic glacier. *Science* 281(5376): 549–551
- Rignot E (2002) Ice-shelf changes in Pine Island Bay, Antarctica, 1947–2000. *Journal of Glaciology* 48(161): 247–256
- Rignot E, Vaughan DG, Schmelz M, Dupont T, MacAyeal D (2002) Acceleration of Pine Island and Thwaites Glaciers, West Antarctica. *Annals of Glaciology* 34: 189–194
- Schmelz M, Rignot E, MacAyeal D (2002) Tidal flexure along ice-sheet margins: comparison of InSAR with an elastic-plate model. *Annals of Glaciology* 34: 202–208
- Schutz BE, Zwally HJ, Shuman CA, Hancock D, DiMarzio JP (2005) Overview of the ICESat Mission. *Geophysical Research Letters* 32 (L21S01), doi: 10.1029/2005GL024009
- Shepherd A, Wingham DJ, Mansley JAD, Corr HFJ (2001) Inland thinning of Pine Island Glacier, West Antarctica. *Science* 291(5505): 862–864
- Shuman CA, Zwally HJ, Schutz BE, Brenner AC, DiMarzio JP, Suchdeo VP, Fricker HA (2006) ICESat Antarctic elevation data: Preliminary precision and accuracy assessment. *Geophysical Research Letters* 33 (L07501), doi: 10.1029/2005GL025227
- Swithinbank C (1988) Antarctica. In: Williams RSjr, Ferrigno, JG (eds) Satellite image atlas of glaciers of the world. United States Geological Survey Professional Paper 1386-B: B1–B278
- Thomas RH, Sanderson TJO, Rose KE (1979) Effect of climatic warming on the West Antarctic ice sheet. *Nature* 277(5695): 355–358
- Thomas RH, Martin TV, Zwally HJ (1983) Mapping ice-sheet margins from radar altimetry data. *Annals of Glaciology* 4: 283–288.
- Vieli A and Payne T (2004) Can the recent thinning and acceleration of Pine Island Glacier, West Antarctica be explained by changes in its ice shelf? AGU miniposter; American Geophys. Union Fall Meeting
- Zwally J et al. (2002) ICESat's laser measurements of polar ice, atmosphere, ocean and land. *Journal of Geodynamics* 34: 405–445.

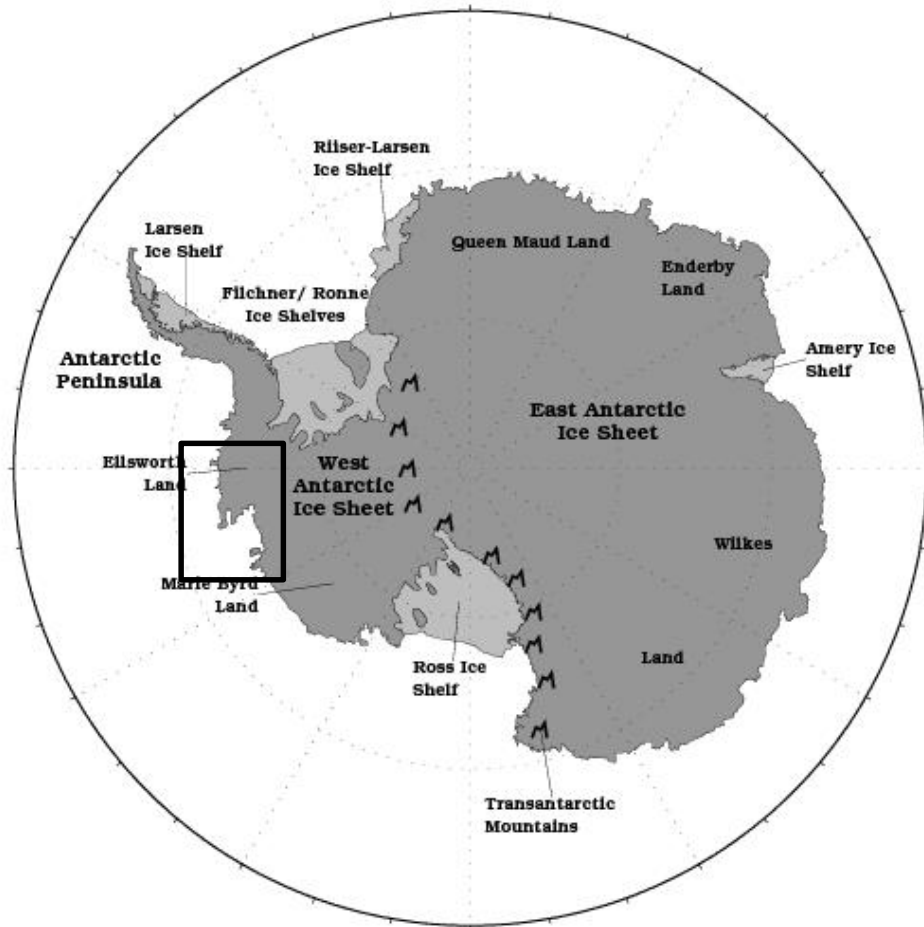


Figure 1: Overview map of Antarctica with location of Walgreen Coast map area marked with box.

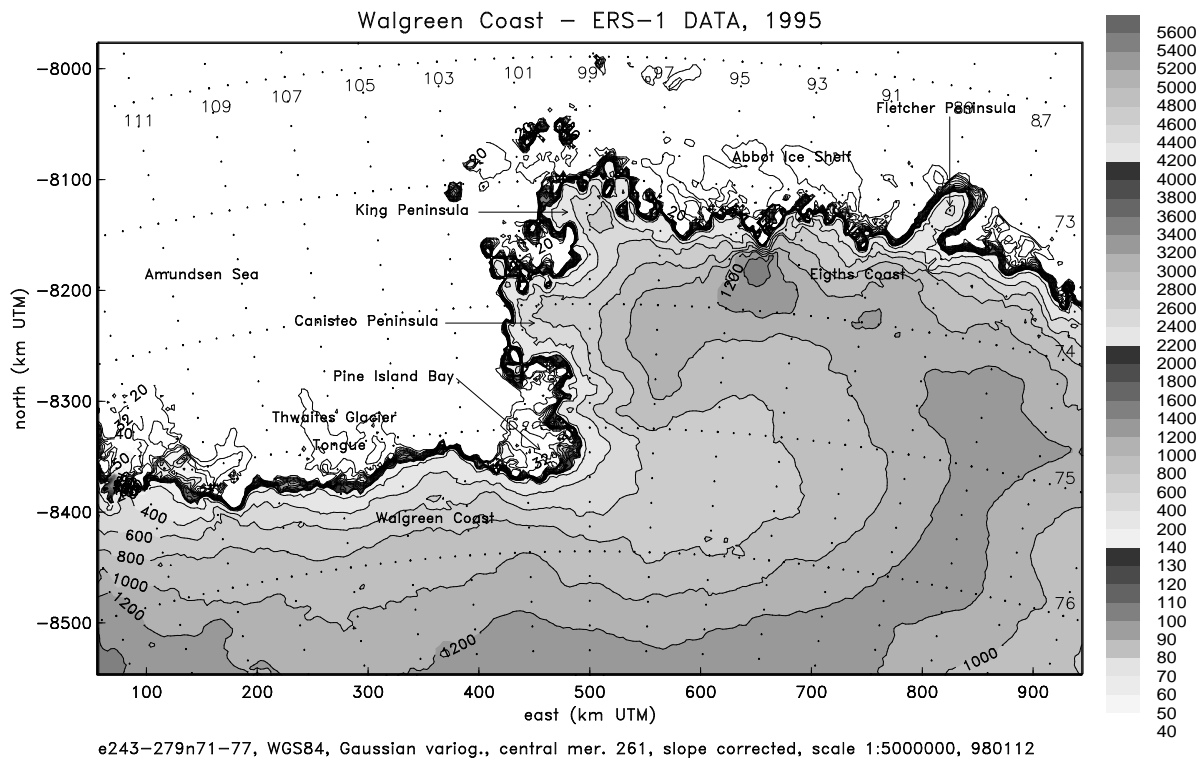


Figure 2: Topographic map of Walgreen Coast m261e243-279n71-77, West Antarctica, based on ERS-1 data from Feb–Aug 1995. Digital elevation model derived using kriging. Elevations in meters above WGS84. Grid resolution 3 km. The abbreviation m261e243-279n71-77 is the Atlas-mapping-scheme reference for map area (117° -81° W/ 71° -77° S), converted to UTM coordinates using middle meridian 261° E, equal to 99° W (see section (3.2) and Herzfeld 2004, p. 198-200).

/data1/ws/pinegl/skripts/m261e243-279n71-77.e.label.coordgrid.totps-U.eps

GLA06-03100414-r1107-L2-2103.P0224-01-00.out ground tracks (100)

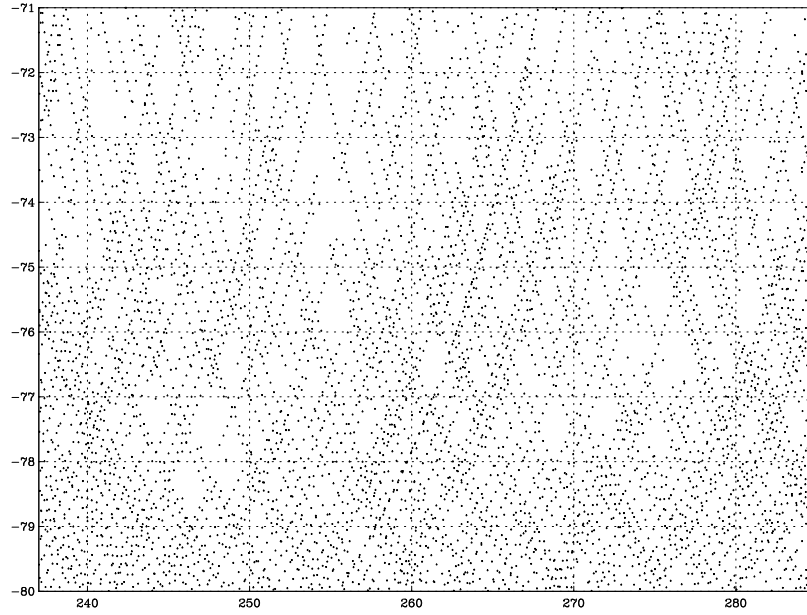
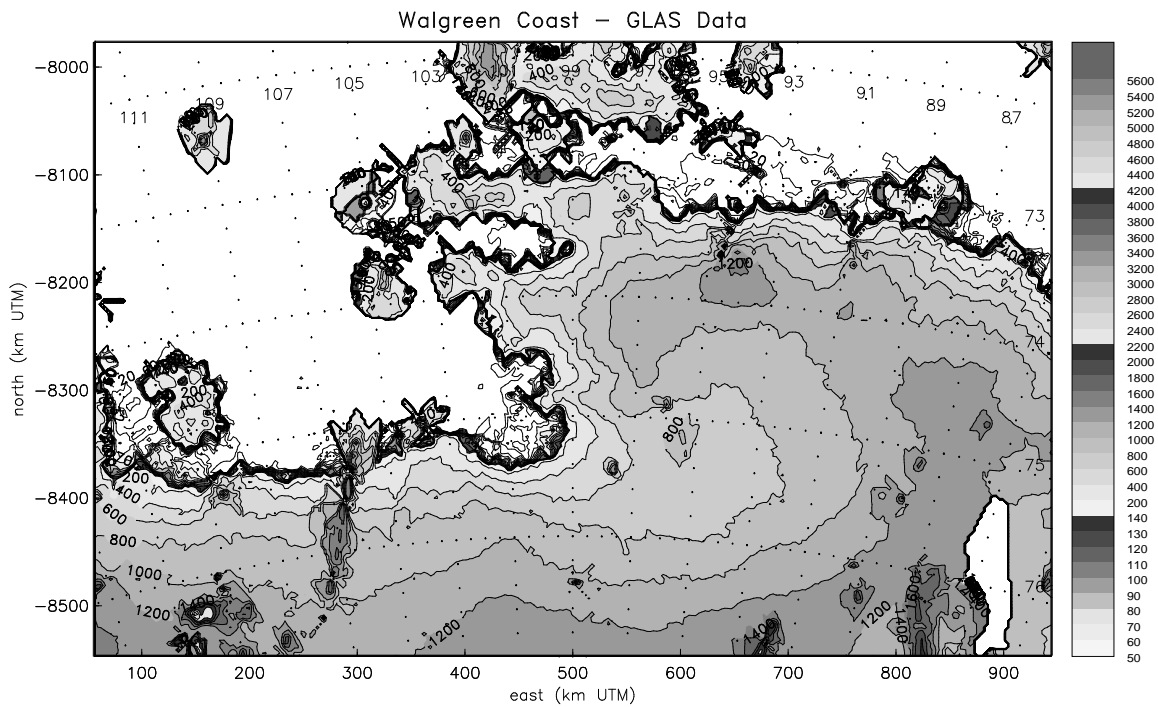


Figure 3: Map of ground locations of laser altimeter data from Laser 2A data (4 Oct–20 Nov 2003), 91 day repeat cycle, for global elevation product GLA06. (Data are subsampled in a regular way to facilitate visualization).

/data1/ws/pinegl/pigglas/rel18/gla06track1.ps



GLA06 Data, (Laser 2A, last33days, rel18), Oct/Nov 2003, vario(350,3450,6000m), search-rg 30km, 1:5000000, last33days.v2.grey

Figure 4: Contoured DEM based on last 33 days of Laser2A (Oct/Nov2003) GLAS data (release 18). DEM derived using ordinary kriging with Gaussian variogram (nug=350, sill 3450, range 6000m). Elevations in meters above WGS84. Note artefacts, eg. over Thwaites Glacier.

/data1/ws/pinegl/pigglas/rel18/gla06/newskript/last33days.v2.grey.coordsgrid.totps

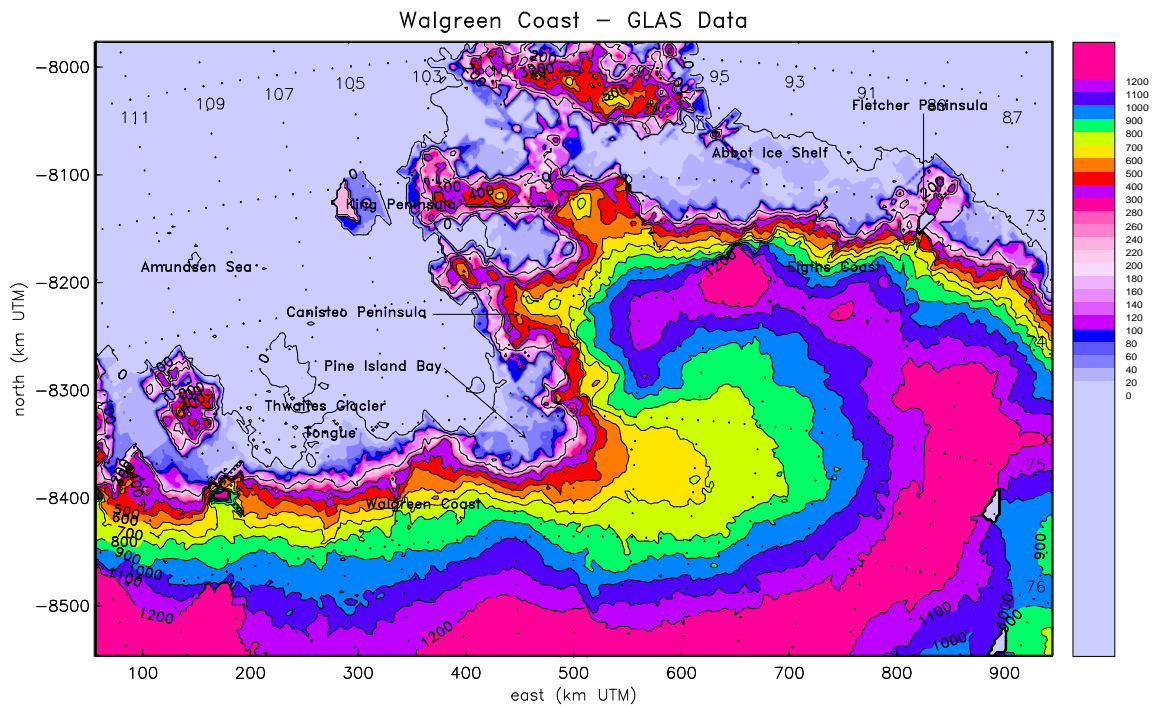


Figure 5: Topographic map of Walgreen Coast m261e243-279n71-77, West Antarctica, based on GLAS data from Oct/Nov 2003. DEM derived using ordinary kriging with Gaussian variogram (nug=350, sill 3450, range 6000m). Elevations in meters above WGS84. Grid resolution 3 km. The abbreviation m261e243-279n71-77 is the Atlas-mapping-scheme reference for map area (117° - 81° W/ 71° - 77° S), converted to UTM coordinates using middle meridian 261° E, equal to 99° W (see section (3.2) and Herzfeld 2004, p. 198-200).

new map:

/data1/ws/pinegl/pigglas/rel18/newgla6/gla06.1.gain.0.col8.coordsgrid.labels.nodate.20080129.totps-U.eps

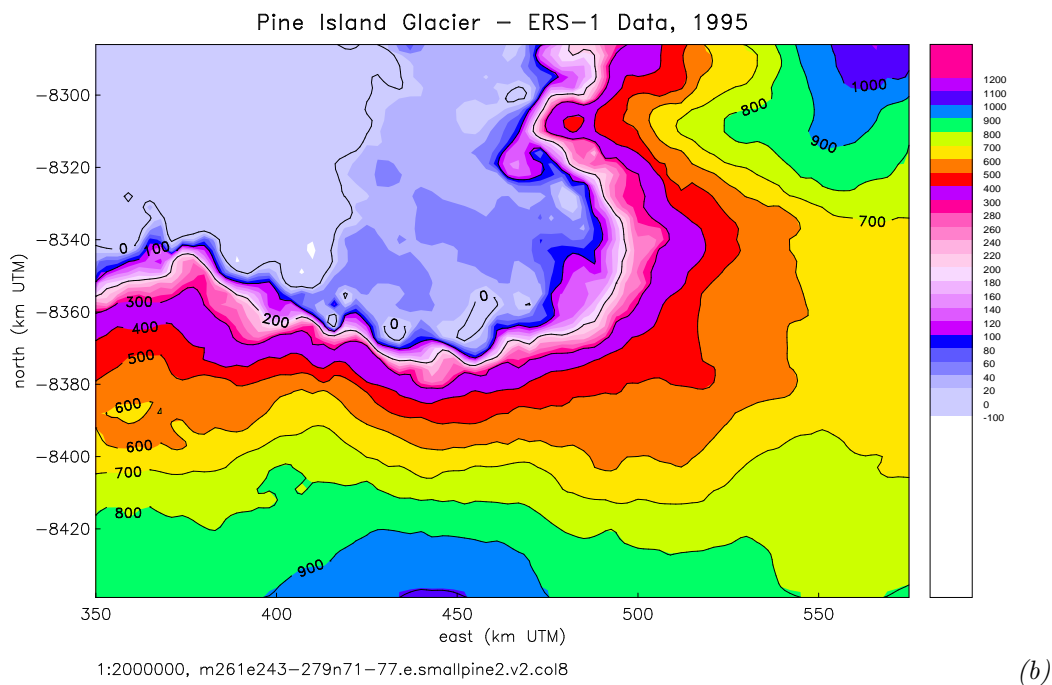
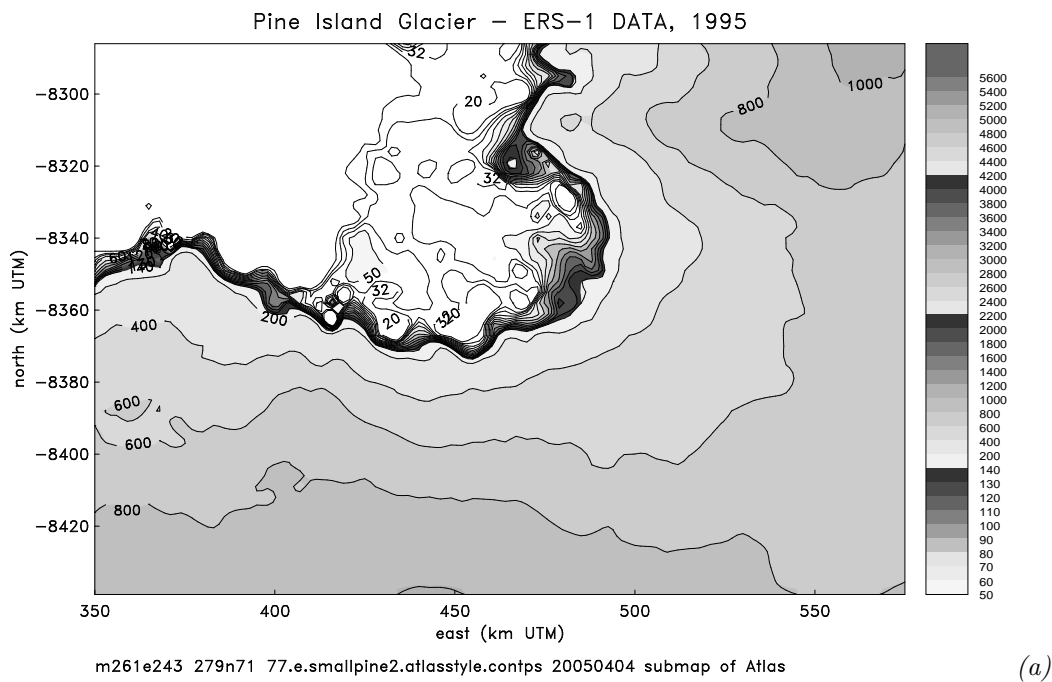
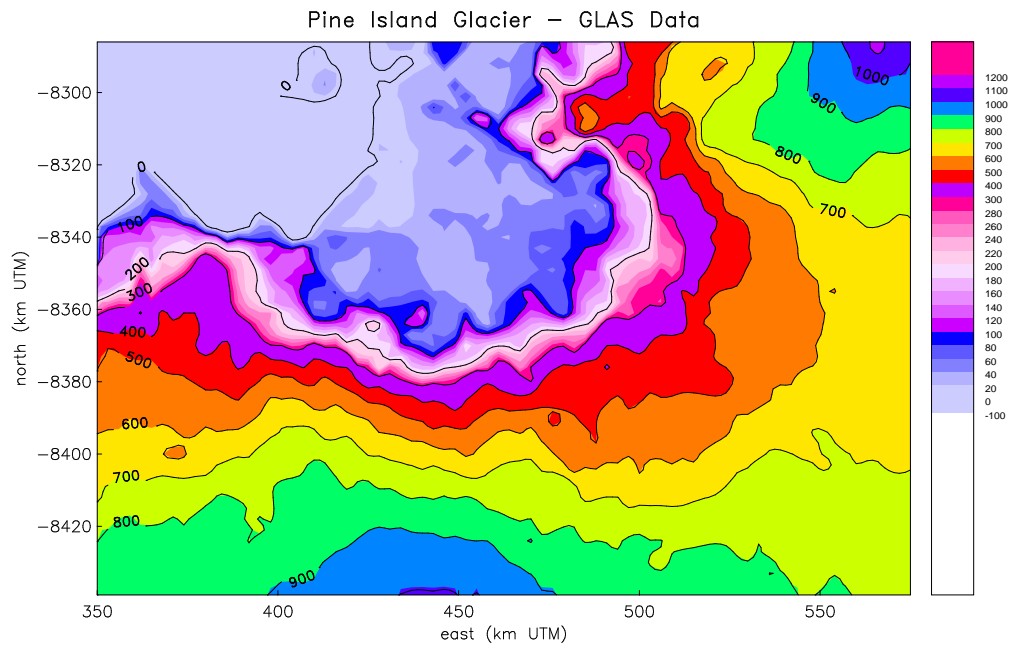
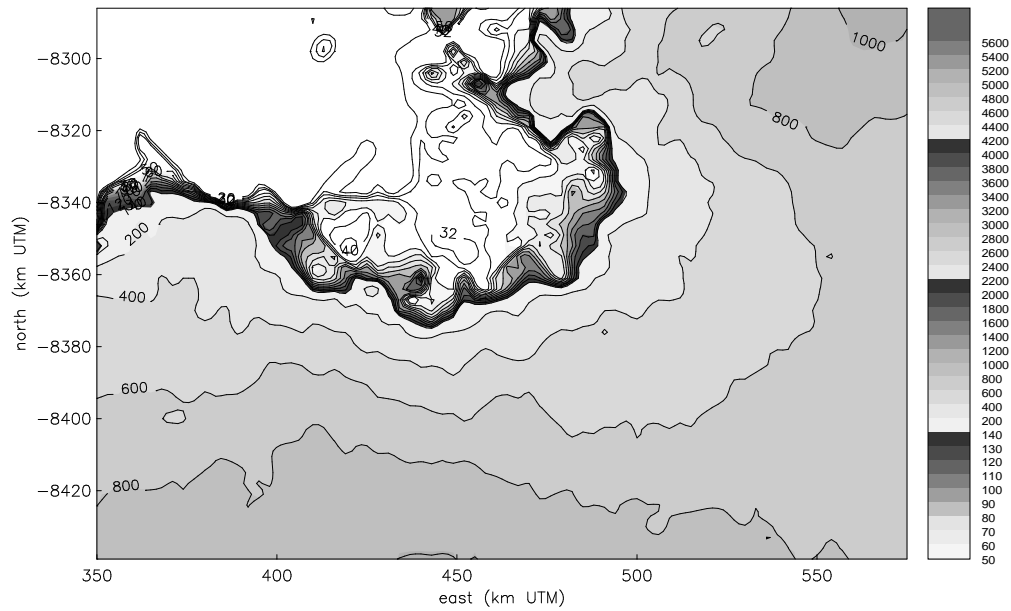


Figure 6: Topographic maps of Pine Island Glacier, based on ERS-1 data from Feb–Aug 1995. DEM derived using kriging. Elevations in meters above WGS84. Grid resolution 3 km. (a) Contour levels and shading designed to enhance surface morphology of floating ice and grounding zone. (b) Contour levels and colors designed to enhance surface elevation.

6a: /data1/ws/pinegl/pigglas/rel18/diffmaps/m261e243-279n71-77.e.smallpine2.atlasstyle.totps

6b: /data1/ws/pinegl/pigglas/rel18/smallpine2/m261e243-279n71-77.e.smallpine2.v2.col8.totps



GLA06 Data, (Laser 2A, gain-crit, rel18), Oct/Nov 2003, vario(350,3450,6000m), search-rg 30km, 1:2000000, gla06.1.gain.smallpine2.v2.col8

Figure 7: Topographic map of Pine Island Glacier, based on GLAS data from Oct/Nov 2003. DEM derived using ordinary kriging with Gaussian variogram (nug=350, sill 3450, range 6000m). Elevations in meters above WGS84. Grid resolution 3 km. (a) Contour levels and shading designed to enhance surface morphology of floating ice and grounding zone. (b) Contour levels and colors designed to enhance surface elevation.

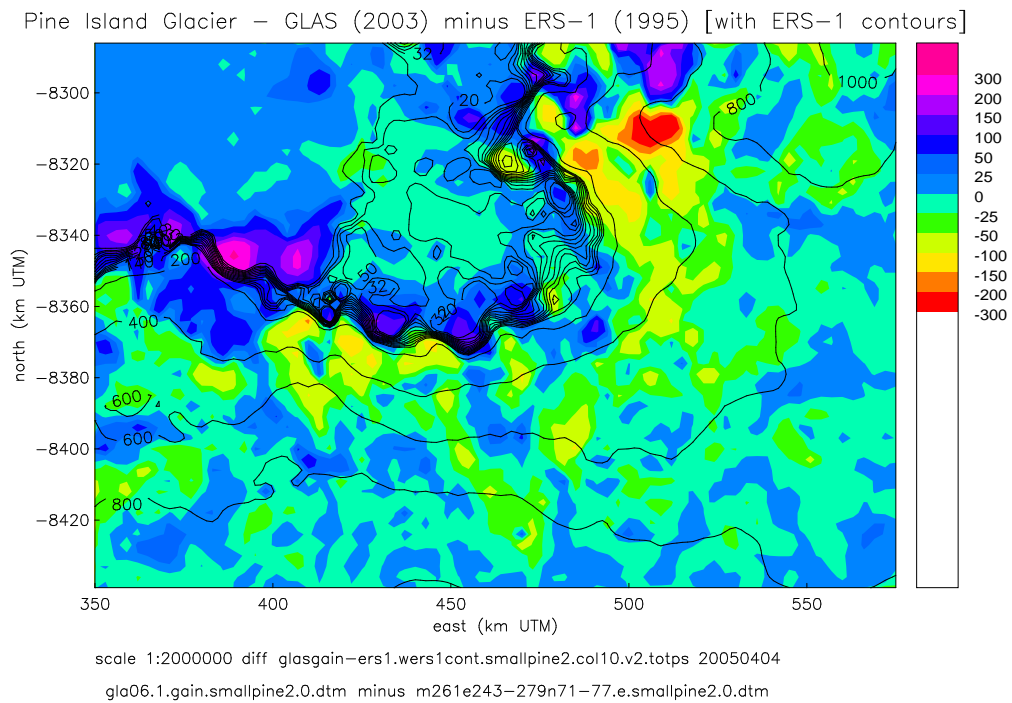


Figure 8: Difference map of Pine Island Glacier DEMs: (2003 GLAS DEM) minus (1995 ERS-1 DEM), with atlasstyle contours of ERS-1 (Fig. 6a) superimposed for geographic reference. Elevation differences in meters.

8: /data1/ws/pinegl/pigglas/rel18/diffmaps/diff-glasgain-ers1.wers1cont.smallpine2.col10.v2.totps

7a: gla06.1.gain.smallpine2.totps (atlasstyle)

7b: /data1/ws/pinegl/pigglas/rel18/gainCriteria/smallpine2/gla06.1.gain.smallpine2.v2.col8.totps